Journal of Applied Electrochemistry **34**: 31–36, 2004.

Water balance in a free-breathing polymer electrolyte membrane fuel cell

TUOMAS MENNOLA[1,*], MATTI NOPONEN[1], TANJA KALLIO[2], MIKKO MIKKOLA[1] and TERO HOTTINEN[1]

[1]*Helsinki University of Technology, Laboratory of Advanced Energy Systems, P.O. Box 2200, 02015 HUT, Finland*
[2]*Helsinki University of Technology, Laboratory of Physical Chemistry and Electrochemistry, P.O. Box 6100, 02015 HUT, Finland*
*(*author for correspondence, fax: +358 9 451 3195, e-mail: tmennola@cc.hut.fi)*

Received 28 March 2003; accepted in revised form 29 July 2003

Key words: anode, current distribution, free-breathing, PEMFC, water balance

Abstract

Water balance in a free-breathing polymer electrolyte membrane fuel cell was studied, focusing on the effect of anode conditions. The methods used were current distribution measurement, water collection from the anode outlet, and the measurement of cell polarization and resistance. Current density levels were 100 and 200 mA cm^{-2}, temperature levels were 40 and 60 °C, and hydrogen stoichiometry range was from 1.5 to 2.5. The direction of hydrogen flow was varied. The fraction of product water exiting through the anode outlet varied from 0 to 58%, and it was found to increase with increasing temperature and hydrogen flow rate. When the general direction of hydrogen flow was against the direction of air flow, the percentage of water removal through the anode was smaller and the current distributions were more even than in the cases where the direction was the same as that of the air flow. This probably resulted from a more favorable distribution of water over the active area. The results also indicate that the net water transport coefficient varies across the active area. In further measurements, operation with the anode side in dead-end mode was investigated. It was also found that water distribution was more favorable when the general direction of hydrogen flow was against the air flow.

1. Introduction

Polymer electrolyte membrane fuel cells (PEMFCs) are becoming a promising power source for small-scale applications. Fuel cells may replace batteries in portable electronic devices, such as laptop computers, and they could be used to power stationary applications outside the electric grid. The development of small fuel cells has progressed at a remarkable rate, but their widespread market introduction still requires further development of the technology. Fuel cell power sources need to be highly reliable in variable ambient conditions, and the system must be miniaturized and simplified. Air supply and water management should preferably be based on the choice of cell geometry and material properties, instead of the use of external devices. Therefore, free convection is a potentially attractive air supply method.

Water balance is a key issue in PEMFC development, because commonly used membrane materials need to be hydrated in order to be proton conductive, and at the same time, excess water must be removed to prevent flooding. Water balance is determined by the water production rate at the cathode and various water transport processes. Water transport in the membrane results from the combined effect of electro-osmotic drag, and diffusion. Electro-osmotic drag transports water to the direction of the migration of the protons, and diffusion results from water activity gradients. The direction of diffusion is usually against the electro-osmotic drag, and therefore, it is often referred to as back-diffusion. Both current and the activity of water may be unevenly distributed over the active area of the cell, and therefore, the magnitude and direction of net water flux may also vary. It can also be expected to be a function of operating parameters, such as temperature, inlet humidities, and stoichiometries. Water transport between the membrane and the gas streams also depends on the choice of cell materials and geometry. In addition, ambient conditions may affect water balance, especially in a free-breathing cell.

Experimental studies on water transport in working fuel cells have been reported by several groups [1–4]. Water transport processes have also been studied by *ex situ* measurements. For example, measurements of electro-osmotic drag in membranes have been reported by several groups, for different membranes and conditions [5–8]. In addition to experimental work, the determination of the net water transport has been among the objectives of several modeling studies [9–30].

Only few experimental studies have been reported on multidimensional water transport characteristics in PEMFCs. Bellows et al. [31] used neutron radiography

technique to study water distribution in membranes. Their results gave indication of the existence of water gradients. Recently Mench et al. [32] determined water distribution by gas chromatographic measurements. According to them, the electro-osmotic drag is almost evenly balanced by back-diffusion in a thin membrane.

Our group has studied mass transport phenomena in free-breathing fuel cells using experimental and modeling methods [33–36]. Our previous work has highlighted the need to understand the net water transport. This gave the motivation to the present study, which aimed at the quantification of net water transport in a free-breathing fuel cell. The measurements were performed using a current distribution measurement system and water collection from the anode outlet. When the results of water balance, current distribution, polarization, and resistance measurements are analyzed together, information can be gained on the possible variation of net water transport across the active area. An additional measurement series was performed with the anode side in dead-end mode. This is an important issue for the development of application-ready fuel cells, for efficiency and safety reasons. Operation in dead-end mode is of particular interest from the point of view of small-scale applications, where it is generally undesirable to have any hydrogen flow exiting the cell.

2. Experimental details

Current distributions were measured using a system built in-house [33]. The system featured a segmented cathode flow-field plate, which enables the measurement of current distribution. The active area of the cell is 50 mm × 50 mm, and the cathode current collector was divided into 12 segments in the horizontal and 4 in the vertical direction. The channel geometry consisted of straight, parallel, vertically oriented channels with ends open to the ambient air. This enables the use of natural convection to drive the air flow.

Commercially available materials and components were used for the rest of the cell. The membrane electrode assembly (MEA) was PRIMEA® 5510 by W.L. Gore & Associates, with 0.3 mg cm^{-2} of Pt per electrode. The gas diffusion layers were SGL CARBON SIGRACET® 10-BB. The anode flow field plate material was graphite, and it was made by GlobeTech, Inc. (now a part of ElectroChem, Inc.). The flow field consisted of parallel serpentine channels. Because the cathode side had straight vertical channels, the result was a cross-flow type local flow pattern over most of the active area.

Other cell components than the cathode flow field plate were not segmented, and a path for electronic current thus existed between the segments through the cathode gas diffusion layer and the electrode. In our previous studies, we have determined that this does not introduce a major error to the measured current distributions, provided that all of the current collector segments are in good contact with the gas diffusion layer. A modeling study on current flow in the gas diffusion layer indicated an error of approximately 15% when a rather extreme change in local current density was assumed between two segments [33]. Under normal conditions, the error should be considerably smaller.

The measurements were performed using a GlobeTech GT-100 Test Station. Cell resistance was measured using a current interrupter circuitry, which is a built-in feature of the load unit. Current distribution data was recorded using an auxiliary data logging system. The ambient temperature and relative humidity were recorded using a Vaisala HMI41 Relative Humidity and Temperature Indicator with an HMP42 probe.

The water balance measurements were performed by collecting water from the anode outlet. Because the cell is free-breathing, it would be difficult to collect water from the cathode outlet without disturbing the operation of the cell. Desiccant, which was $CaSO_4$-based Driedrite®, was placed in a glass tube, and the anode outlet gas was led through it. The tube between the anode outlet and the desiccant tube was heated to prevent condensation. The amount of water exiting the cell through the anode outlet was determined by weighing the desiccant before and after a measurement run. The duration of the measurements was 4 h unless otherwise noted in the discussion of the results. It was preceded by a 1 h stabilization period under the same current density and operating conditions.

For the second measurement series, in which the cell was operated in dead-end mode, a shutoff valve was installed downstream of the cell. By closing the valve, the cell was forced to operate on a stoichiometric amount of hydrogen. The durations of the measurement and stabilization periods were the same as in the first series.

3. Results and discussion

3.1. *Net water transport*

The measurements were performed at cell temperatures of 40 and 60 °C. At the higher temperature, the current density levels were 100 and 200 mA cm^{-2}. At 40 °C, the higher current density resulted in unstable performance, and therefore, this case was excluded from the data set. At each temperature and current density level, hydrogen stoichiometry was varied. The stoichiometries were 1.5, 2.0, and 2.5. In addition, each measurement was performed using two different directions of hydrogen flow. These were designated ‘down’ and ‘up’. However, these should be understood only as descriptions of the general direction of hydrogen flow in the anode flow field. For example, direction ‘down’ thus implies that hydrogen entered from an upper corner of the active area, flowed through the serpentine-type flow field, and exited from the opposite lower corner. On the cathode side, the rate of air flow was not directly controllable, and no attempt was made to measure it. Our modeling

studies on the same channel geometry and operating parameters indicate an upward velocity of approximately 0.01–0.03 m s^{-1} [36].

An exception to the normal measurement procedure was the set of operating parameters $T_{cell} = 60$ °C, $j_{ave} = 200$ mA cm^{-2}, and hydrogen flow direction up. High water flux made it necessary to shorten the water collection period to 3 h. At $T_{cell} = 60$ °C and $j_{ave} = 100$ mA cm^{-2}, severe drying occurred when hydrogen flow direction was up, and therefore, this combination of parameters was excluded from the series.

The net water transport was calculated from the collected amount of water and the total water production, which was obtained from Faraday's law. It was assumed that water did not accumulate inside the cell. The percentages were calculated using the assumption that the collected water originated entirely from the cathode reaction. This should be a good approximation, because the amount of water vapor entering the cell through the cathode inlet was small. The contribution of ambient humidity to water vapor pressure in the cathode channels can be calculated from the measured temperatures and relative humidities of ambient air. The ambient temperature during the measurements varied from 19.8 to 21.5 °C, and the relative humidity of ambient air varied from 10.5 to 21.2%. The contribution of ambient humidity to the humidity level in the cathode channels, expressed as percentage points of relative humidity, is 8% or less at 40 °C, and 2% or less at 60 °C.

The results are given in Figures 1 and 2 as percentages of product water exiting through the anode outlet at $T_{cell} = 40$ °C, $j_{ave} = 100$ mA cm^{-2} and $T_{cell} = 60$ °C, $j_{ave} = 200$ mA cm^{-2}, respectively. At $T_{cell} = 60$ °C, $j_{ave} = 100$ mA cm^{-2}, a measurable amount of water was collected only at the highest stoichiometry. It was found to be 2% of the total water production.

Net water flux is commonly described using the net water transport coefficient α, which is defined as the

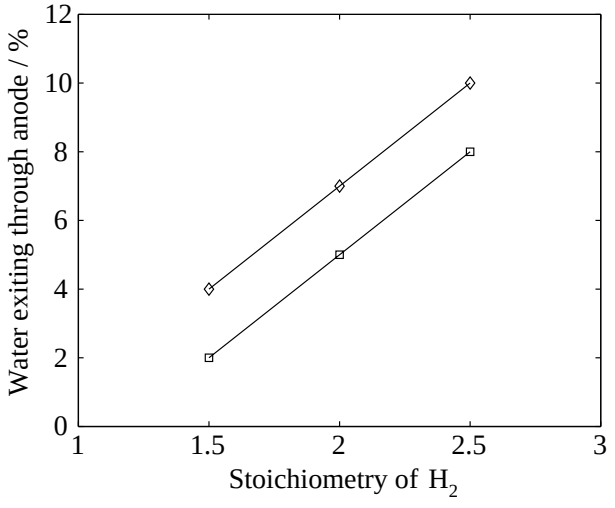

Fig. 1. Percentage of water exiting the cell through the anode outlet: $T_{cell} = 40$ °C, $j_{ave} = 100$ mA cm^{-2}, general flow directions of hydrogen up (◇) and down (□).

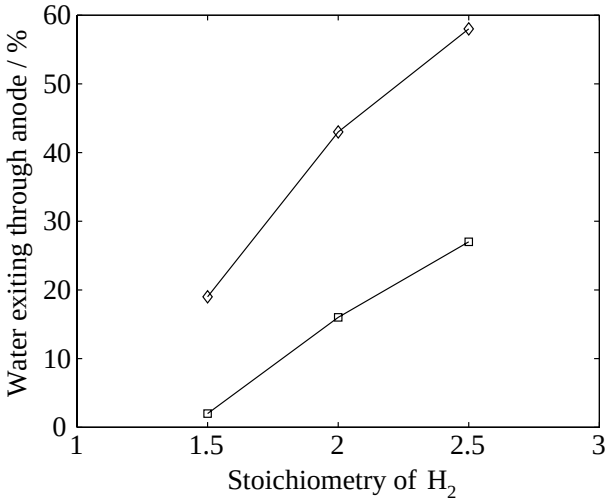

Fig. 2. Percentage of water exiting the cell through the anode outlet: $T_{cell} = 60$ °C, $j_{ave} = 200$ mA cm^{-2}, general flow directions of hydrogen up (◇) and down (□).

average number of water molecules transported from the anode to the cathode per proton. Expressed as α, the range of net water transport depicted in Figure 1 is from −0.01 to −0.05. In Figure 2, the range is from −0.01 to −0.29. A negative value of α implies that the direction is toward the anode.

It can be seen that net water transport is strongly influenced by the anode conditions. Water transport toward the anode increases with increasing hydrogen flow rate, because a higher flow rate enables more water to evaporate into the gas flow. In both of the depicted cases, water flux at the anode outlet was lower when the direction of hydrogen flow was down.

The results can be understood by considering the distribution of water and the variation of α across the active area. The relative humidity of air can be assumed to increase toward the upper ends of the cathode channels. When dry hydrogen enters the cell from the upper corner, there is a high flux of water toward the anode in the upper parts of the cell, as a result of the steep water activity gradient across the membrane. Some water is thus transported with the hydrogen flow to the lower parts of the anode compartment. On the other hand, water activity is low near the inlets of the cathode channels. As a result, in the lower parts of the cell, the magnitude of water transport from the cathode to the anode decreases, and its direction may even be reversed. When the direction of hydrogen flow is up, this redistribution of water inside the cell does not take place. The water evaporated into the hydrogen flow in the upper parts of the cell simply exits the cell, resulting in a higher fraction of water removal through the anode.

3.2. *Current distribution*

Current distributions averaged in the horizontal direction are depicted in Figures 3–5. The locations of the data points represent the center points of the segments,

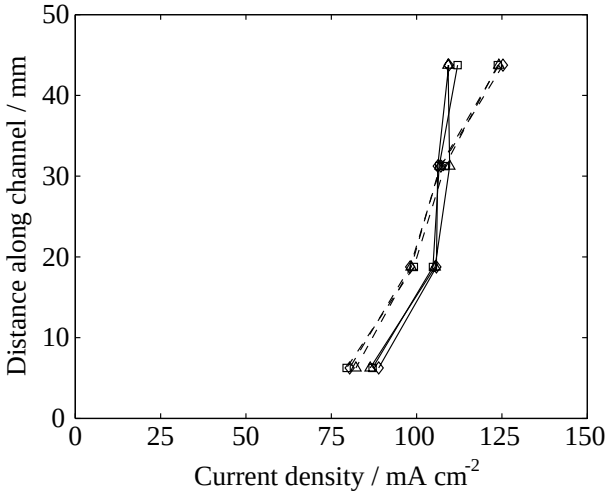

Fig. 3. Current distributions averaged in the horizontal direction. Stoichiometries of hydrogen 1.5 (□), 2.0 (◇) and 2.5 (△), general directions of hydrogen flow up (- - -) and down (—). $T_{cell} = 40$ °C, $j_{ave} = 100$ mA cm^{-2}.

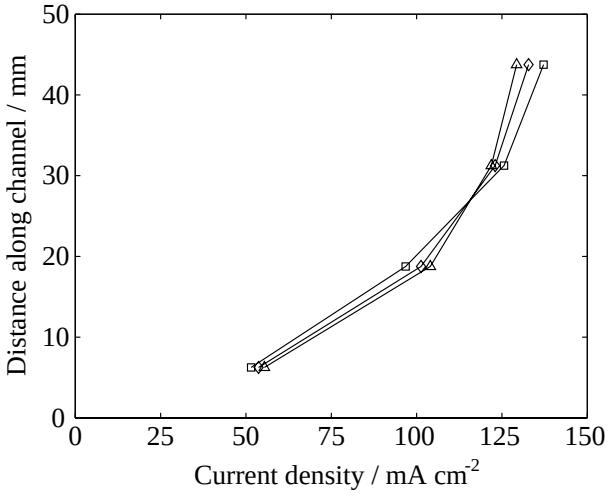

Fig. 4. Current distributions averaged in the horizontal direction. Stoichiometries of hydrogen 1.5 (□), 2.0 (◇) and 2.5 (△), general direction of hydrogen flow down. $T_{cell} = 60$ °C, $j_{ave} = 100$ mA cm^{-2}.

and the points in each distribution have been connected with lines to guide the eye.

At $T_{cell} = 40$ °C, the effect of hydrogen stoichiometry and flow direction was moderate, as shown in Figure 3. When the flow direction was up, the current distribution became slightly more uneven. This indicates some local drying in the lower parts of the cell, which also explains the difference in the amount of collected water. Figure 4 shows the current distributions at $T_{cell} = 60$ °C and $j_{ave} = 100$ mA cm^{-2}. It is evident that drying was taking place in the lower parts of the cell, which resulted from an increase of evaporation on the cathode side. It appears that water redistribution by hydrogen flowing down was not sufficient to maintain the proton conductive phases fully humidified. Consequently, hydrogen exited the cell nearly dry, as indicated by the water collection measurements. The current distributions at

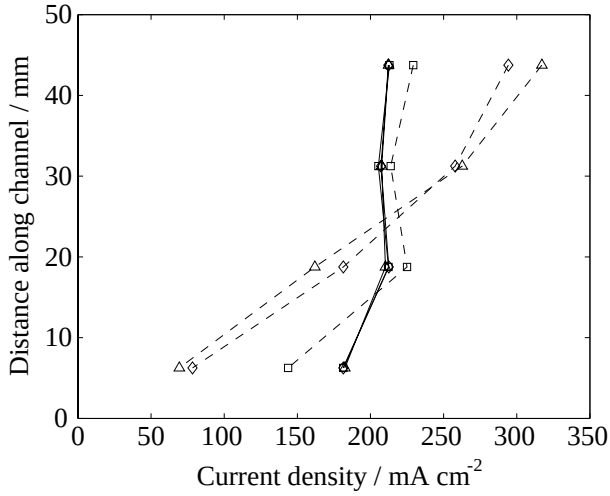

Fig. 5. Current distributions averaged in the horizontal direction. Stoichiometries of hydrogen 1.5 (□), 2.0 (◇) and 2.5 (△), general directions of hydrogen flow up (- - -) and down (—). $T_{cell} = 60$ °C, $j_{ave} = 200$ mA cm^{-2}.

$T_{cell} = 60$ °C and $j_{ave} = 200$ mA cm^{-2} are depicted in Figure 5. When hydrogen flow direction was down, the current distributions were relatively even. This supports the conclusion that water originating from the upper parts of the cell improved humidification in the lower parts. Reversing the hydrogen flow resulted in a highly uneven current distribution, because the combination of high temperature and dry gases on both sides of the membrane caused significant local drying in the lower parts of the cell.

3.3. *Cell polarization and resistance*

The cell voltages and area-specific resistances recorded during the water collection measurements are depicted in Figures 6 and 7, respectively. The figures indicate that

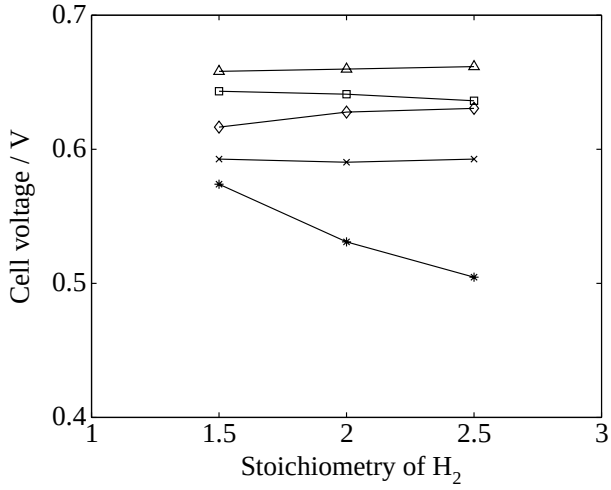

Fig. 6. Cell voltage: $T_{cell} = 40$ °C, $j_{ave} = 100$ mA cm^{-2}, H_2 down (□); $T_{cell} = 40$ °C, $j_{ave} = 100$ mA cm^{-2}, H_2 up (◇); $T_{cell} = 60$ °C, $j_{ave} = 100$ mA cm^{-2}, H_2 down (△); $T_{cell} = 60$ °C, $j_{ave} = 200$ mA cm^{-2}, H_2 down (×); $T_{cell} = 60$ °C, $j_{ave} = 200$ mA cm^{-2}, H_2 up (∗).

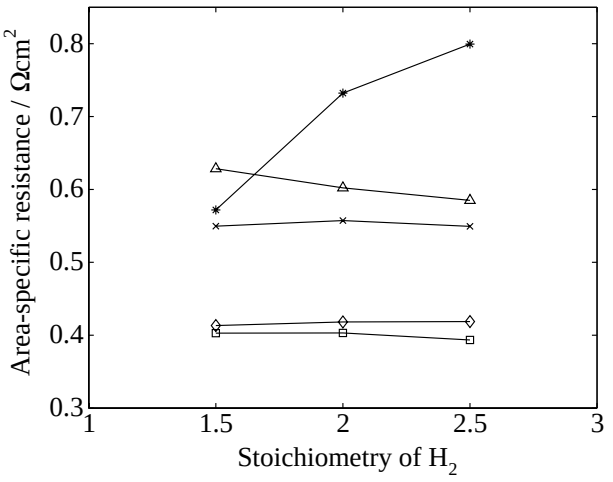

Fig. 7. Area-specific resistance: $T_{cell} = 40$ °C, $j_{ave} = 100$ mA cm^{-2}, H_2 down (□); $T_{cell} = 40$ °C, $j_{ave} = 100$ mA cm^{-2}, H_2 up (◇); $T_{cell} = 60$ °C, $j_{ave} = 100$ mA cm^{-2}, H_2 down (△); $T_{cell} = 60$ °C, $j_{ave} = 200$ mA cm^{-2}, H_2 down (×); $T_{cell} = 60$ °C, $j_{ave} = 200$ mA cm^{-2}, H_2 up (∗).

performance was better when the hydrogen flow direction was downward. However, at $T_{cell} = 40$ °C, the effect of anode conditions was relatively small. At the higher temperature level, resistance was higher as a result of drying in some parts of the cell. The current distributions in Figures 4 and 5 indicate that the most severe drying took place in the lower parts of the active area. This was especially obvious at 200 mA cm^{-2} and flow direction up. With this combination of operating parameters, an increase of resistance with increasing flow rate was observed. It is also worth noting that an increase in average current density lowered the cell resistance slightly when the direction of hydrogen flow was down. This again is an indication of the redistribution of water inside the cell.

3.4. *Anode in dead-end mode*

Another measurement series was performed in order to investigate the performance of the cell in dead-end mode. For this measurement series, the cell was reassembled with a new MEA and gas diffusion layers. The levels of cell temperature and average current density were the same as in the previous series. The measurements were performed with hydrogen flow directions of both down and up.

The voltages and area-specific resistances in dead-end mode are summarized in Table 1. The ambient temperature varied between 19.7 and 21.9 °C, and the relative humidity of ambient air varied between 8.4 and 21.9%. The current distributions are depicted in Figure 8. Comparison with the previous measurement series reveals that the drying problems encountered in the previous series were now less severe, resulting in higher current densities near the lower edge of the active area. At $T_{cell} = 60$ °C and $j_{ave} = 100$ mA cm^{-2}, the flow direction up was now found to result in stable perfor-

Table 1. Cell voltage and area-specific resistance; anode in dead-end mode

T_{cell} /°C	J_{ave} /mA cm^{-2}	H_2 flow direction	U/V	r /Ω cm^2
40	100	Down	0.687	0.35
40	100	Up	0.704	0.35
60	100	Down	0.668	0.39
60	100	Up	0.637	0.61
60	200	Down	0.610	0.49
60	200	Up	0.687	0.53

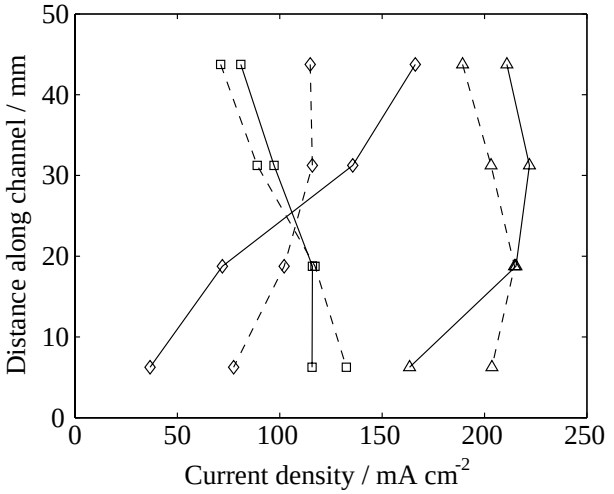

Fig. 8. Current distributions averaged in the horizontal direction. $T_{cell} = 40$ °C, $j_{ave} = 100$ mA cm^{-2} (□); $T_{cell} = 60$ °C, $j_{ave} = 100$ mA cm^{-2} (◇); $T_{cell} = 60$ °C, $j_{ave} = 200$ mA cm^{-2} (△). Anode in dead-end mode, general directions of hydrogen flow down (- - -) and up (—).

mance, contrary to the previous series, in which the same combination of parameters caused severe drying. Apparently, the reduced hydrogen flow rates resulted in the alleviation of drying problems in the cases where the hydrogen flow direction was up. It is also possible that temperature distribution was different from the previous series, because the location of the temperature sensor in the anode flow field plate was slightly altered when the cell was reassembled. Because of the high thermal conductivity of graphite, the location of the sensor should not affect the temperature distribution significantly. However, the saturation pressure of water vapor is strongly dependent on temperature, and therefore, water balance is sensitive to changes in temperature. Some caution should thus be exercised when comparing the two series.

Comparison of the distributions recorded using different hydrogen flow directions indicates trends similar to those observed in the previous series. At 40 °C, the difference between results at the two flow directions is relatively small. At 60 °C and $j_{ave} = 100$ mA cm^{-2}, the effect of water redistribution can be clearly observed from the difference between the current distributions obtained with different flow directions. At the higher current density level, the difference is slightly less

pronounced, probably resulting from improved humidification as an outcome of higher water production.

4. Conclusions

The percentage of water removed through the anode varied from 0 to 58%. It was found to increase with increasing temperature and hydrogen flow rate. When the general direction of hydrogen flow was against the direction of air flow, the percentage of water removal through the anode was always smaller than when the general direction of hydrogen flow had the same direction as the air flow. Inspection of the rest of the measurements reveals that when the direction of hydrogen flow was against the air flow, the current distributions were more even, cell voltage was higher, and resistance was lower than when the direction of hydrogen flow was the same as that of the air flow. These observations indicate that in the former case, water was favorably redistributed inside the cell, whereas in the latter case, performance of the lower parts of the cell suffered from drying of the proton conductive phases. It thus appears that the variation of the water transport coefficient over the active area must be considered to explain the results. Current distribution measurements offer an indirect way to gain information about local water balance, because water production is directly proportional to current density and local current density is affected by humidification conditions.

In further measurements with the anode side in dead-end mode, the variation of the hydrogen flow direction had similar effects as in the measurement series in which the hydrogen flow was overstoichiometric. This indicates that the redistribution of water was taking place when the general direction of hydrogen flow was down, despite the lower flow rate.

Acknowledgements

Financial support for this work was provided by: The National Technology Agency of Finland (Tekes), The Nordic Energy Research Program (NEFP), The Academy of Finland, and the Fortum Foundation. Gas diffusion materials were provided by SGL Technologies GmbH, Germany, affiliate of SGL CARBON GROUP.

References

1. F.N. Büchi and S. Srinivasan, *J. Electrochem. Soc.* **144** (1997) 2767.
2. D. Picot, R. Metkemeijer, J.J. Bezian and L. Rouveyre, *J. Power Sources* **75** (1998) 251.
3. K.-W. Choi, D.-H. Peck, C.S. Kim, D.-R. Shin and T.-H. Lee, *J. Power Sources* **86** (2001) 197.
4. G.J.M. Janssen and M.L.J. Overvelde, *J. Power Sources* **101** (2001) 117.
5. T.F. Fuller and J. Newman, *J. Electrochem. Soc.* **139** (1992) 1332.
6. T.A. Zawodsinski, C. Derouin, S. Radzinski, R.J. Sherman, V.T. Smith, T.E. Springer and S. Gottesfeld, *J. Electrochem. Soc.* **140** (1993) 1041.
7. T.A. Zawodzinski, J. Davey, J. Valerio and S. Gottesfeld, *Electrochim. Acta* **40** (1995) 297.
8. M. Ise, K.D. Kreuer and J. Maier, *Solid State Ionics* **125** (1999) 213.
9. T.E. Springer, T.A. Zawodsinski and S. Gottesfeld, *J. Electrochem. Soc.* **138** (1991) 2334.
10. T.V. Nguyen and R.E. White, *J. Electrochem. Soc.* **140** (1993) 2178.
11. M. Wöhr, K. Bolwin, W. Schurnberger, M. Fischer, W. Neubrand and G. Eigenberger, *Int. J. Hydrogen Energy* **23** (1998) 213.
12. T. Okada, G. Xie, O. Gorseth, S. Kjelstrup, N. Nakamura and T. Arimura, *Electrochim. Acta* **43** (1998) 3741.
13. P. Futerko and I.-M. Hsing, *Electrochim. Acta* **45** (2000) 1741.
14. K. Dannenberg, P. Ekdunge and G. Lindbergh, *J. Appl. Electrochem.* **30** (2000) 1377.
15. S. Dutta, S. Shimpalee and J.W. Van Zee, *Int. J. Heat Mass Transfer* **44** (2001) 2029.
16. D.M. Bernardi and M. Verbrugge, *AIChE J.* **37** (1991) 1151.
17. D.M. Bernardi and M. Verbrugge, *J. Electrochem. Soc.* **139** (1992) 2477.
18. V. Gurau, H. Liu and S. Kakaç, *AIChE J.* **44** (1998) 2410.
19. M. Eikerling, Yu.I. Kharkats, A.A. Kornyshev and Yu.M. Volfkovich, *J. Electrochem. Soc.* **145** (1998) 2684.
20. D. Singh, D.M. Lu and N. Djilali, *Int. J. Eng. Sci.* **37** (1999) 431.
21. S. Um, C.-Y. Wang and K.S. Chen, *J. Electrochem. Soc.* **147** (2000) 4485.
22. G. Murgia, L. Pisani, M. Valentini and B. D'Aguanno, *J. Electrochem. Soc.* **149** (2002) A31.
23. N. Djilali and D. Lu, *Int. J. Therm. Sci.* **41** (2002) 29.
24. T.F. Fuller and J. Newman, *J. Electrochem. Soc.* **140** (1993) 1218.
25. A.C. West and T.F. Fuller, *J. Appl. Electrochem.* **26** (1996) 557.
26. G.J.M. Janssen, *J. Electrochem. Soc.* **148** (2001) A1313.
27. K. Dannenberg, P. Ekdunge and G. Lindbergh, *J. Appl. Electrochem.* **30** (12) (2000) 1377.
28. P.J.S. Vie, dissertation 'Characterisation and Optimisation of the Polymer Electrolyte Fuel Cell', Norges teknisk-naturvitenskapelige universitet, Norway (2002).
29. A. Rowe and X. Li, *J. Power Sources* **102** (2001) 82.
30. L. You and H. Liu, *Int. J. Heat and Mass Transfer* **45** (2002) 2277.
31. R.J. Bellows, M.Y. Lin, M. Arif, A.K. Thompson and D. Jacobson, *J. Electrochem. Soc.* **146** (1999) 1099.
32. M.M. Mench, Q.L. Dong and C.Y. Wang, In situ water distribution measurements in an operating polymer electrolyte fuel cell, to appear *in* J.W. Van Zee, M. Murthy, T.F. Fuller and S. Gottesfeld (Eds), Proceedings of the 202nd meeting of the Electrochemical Society: 'Proton Conducting Membrane Fuel Cells III', (2003).
33. M. Noponen, T. Mennola, M. Mikkola, T. Hottinen and P. Lund, *J. Power Sources* **106** (2002) 304.
34. M. Noponen, T. Hottinen, T. Mennola, M. Mikkola and P. Lund, *J. Appl. Electrochem.* **32** (2002) 1081.
35. T. Hottinen, M. Noponen, T. Mennola, O. Himanen, M. Mikkola and P. Lund, *J. Appl. Electrochem.* **33** (2003) 265.
36. T. Mennola, M. Noponen, M. Aronniemi, T. Hottinen, M. Mikkola, O. Himanen and P. Lund, *J. Appl. Electrochem.* **33** (2003) 979.